On Solving Inverse Problems for Electric Fish Like Robots

M. Alamir, O. Omar, N. Servagent, A. Girin, P. Bellemain, V. Lebastard, P. B. Gossiaux, F. Boyer and S. Bouvier

***Abstract*— This paper relates preliminary results concerning the solution of inverse problems arising in electric sense based navigation. This sense is used by electric fishes to move in dark waters using the electric current measurements perceived by the epidermal sensors as these are affected by the presence of obstacles. The latter change the resulting induced measures by instantaneously disturbing the fish self-produced electric field. The approach lies on a recently proposed graphical signature based classification methodology to overcome the computational burden associated to an explicit inversion of the mathematical equations. A preliminary validation of the proposed solution is obtained using a dedicated experimental setting.**

I. INTRODUCTION

The ability of weakly electric fishes to hunt and navigate without visual cues has been recognized long time ago [1], [2]. Researchers effort to understand the underlying electrolocation mechanism enabled to establish that this is done by perceiving the effects of self-produced electric signals by means of epidermal electroreceptors. The signal received by these receptors depends on the environment configuration (presence of objects, their electrical properties, their size, their form and so on).

More recently, the idea of using this electrolocation principle on-board of underwater robots emerged [3] since it shows several advantages. Indeed, beyond the possibility of exploring dark waters without visual cues, the instantaneous character of the electrical sense (when compared to sonar-based solutions) suggests the possibility to reproduce reflex-like behavior in such robots. Moreover, the possibility to use different electrical voltage profiles opens the way to a sort of active redundancy-based investigation that can be precious in the presence of ambiguities as for the perception of the environment by the robot.

The French ANR-RAAMO project aims at conducting researches leading to an eel-like robot capable of electrolocation. In particular, several electrosensory arrays have been developed together with a simplified experimental facility that serves for validation purposes. The latter concern both the modeling approach of the underlying electrolocation equations (direct equations) but also the algorithms that aim at reconstructing the information on the environment based on the available measurements (inverse problems). More precisely, the direct problem needs the Laplace equation

$$\Delta U = 0$$

to be solved where U is the potential that defines the electric fields through $\mathbf{E} = -\nabla U$ (irrotational nature of the field in the quasi-stationary regime). The solution of the Laplace's law needs the boundary conditions to be defined according to the properties of the objects that are immersed in the environment near the electro-sensor probe [8]. These boundary conditions involve either U or its normal slope ($\frac{\partial U}{\partial n}$) on the nodes that belong to the boundary of the domain (which includes the boundary of the objects). the direct solution of the electrolocation equations needs a rather involved numerical burden (Boundary elements method for instance) that yields a system of equations that takes the following form:

$$\Big[A(\textit{config})\Big] \begin{pmatrix} \bar{U} \\ \bar{I} \end{pmatrix} = B(\textit{config}) \tag{1}$$

$$\text{Measurement vector} = C \begin{pmatrix} \bar{U} \\ \bar{I} \end{pmatrix} \tag{2}$$

where *config* shortly denotes all the parameters that completely describe the configuration of the environnement while $(\bar{U}, \bar{I})$ are the vectors of voltage and current at each node of the discretization mesh. Note that the B vector gathers those potentials and currents that are known or are imposed on some specific frontiers (sensors, bodies of given characteristics).

It is a fact that except for very simple cases [7], solving the inverse problems

$$\textit{config} = \mathcal{F}(\textit{Measurement})$$

which is a high dimensional, nonlinear and hybrid problem is extremely hard and doing this in real-time is unrealistic. That is the reason why the use of model-free inversion algorithms has to be seriously investigated. This is the aim of the present contribution that relates some preliminary experimentally assessed results on the use of such a model-free approach to solve a specific electrolocation problem.

This paper is organized as follows: first, section II presents the experimental facility together with the specific

This work was supported by the French ANR-RAAMO Project and the European Project ANGELS

M. Alamir and O. Omar are with Gipsa-lab, University of Grenoble. BP 46, Domaine Universitaire, 38402 Saint Martin d'Hères, France. mazen.alamir(oumayma.omar)@gipsa-lab.inpg.fr

N. Servagent, P. B. Gossiaux and S. Bouvier are with SUBATECH, UMR 6457, Ecole des Mines de Nantes, CNRS-IN2P3, Université de Nantes, La Chantrerie - 4, rue Alfred Kastler B.P. 20722 - F-44307 NANTES Cedex 3

F. Boyer, A. Girin and V. Lebastard are with IRCCyN, Ecole des Mines de Nantes, La Chantrerie - 4, rue Alfred Kastler B.P. 20722 - F-44307 NANTES Cedex 3

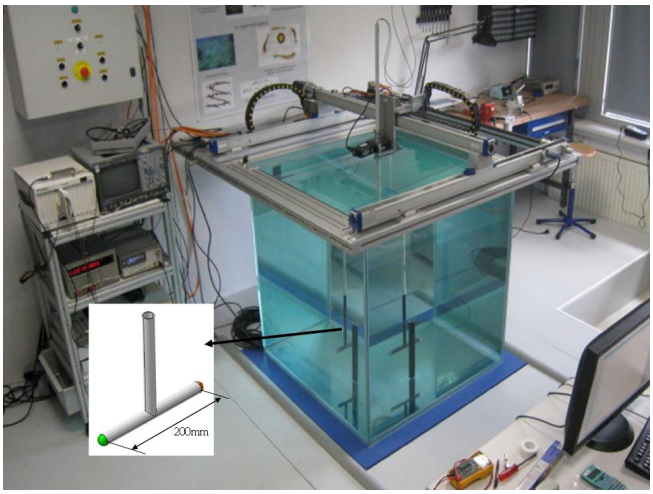

Fig. 1. Photo of the experimental facility available at SUBATECH. One can recognize the position/orientation control plate-form for the electro-sensor probe. This enables a controlled movement of the probe in the aquarium to be performed in order to collect the resulting electrosensing measurements.

electrolocation problem to be addressed. Section III describes the general framework that underlines the proposed solution while section IV shows the experimental validation results.

II. ELECTROLOCATION EXPERIMENTAL FACILITY

In order to start investigation on a simpler problem than the one corresponding to a fully instrumented swimming robot, the RAAMO Project partners developed the experimental facility depicted in Figure 1 where a schematic view of a two-electrodes (inox 316) probe can be viewed. This probe is immersed in an aquarium at coordinates (x, y), mid-height, and angular position θ that are tightly controlled using respectively a cartesian robot and a precise rotating stage. While in the forthcoming experimental investigation, only the two electrodes probe has been used, it is worth mentioning that several versions of the probe are also available that contain up to 16 electrodes, distributed over 4 groups of four electrodes.

The electrolocation problem can be stated as follows:

> *define an actuation protocole, a learning scheme and the corresponding inverse problem solver that enable the probe to determine its coordinates (x, y) from the only electrolocation related measurement.*

It goes without saying that many actuation protocoles can be imagined and the one proposed here is just a particular choice among many other possible ones.

Regardless the actuation protocole being used, this protocole has to lead to a measured signal profile that enables the position (x, y) to be discriminated by *manipulating* the resulting measurement and this, regardless the initial value of the angular position θ. In other words, one must be at least able by observing the measurement profile to decide whether the probe is near a wall, in the center of the aquarium or near a corner. In a sense, the inverse problem can be viewed as a measurement-based *classification* problem. Nevertheless, it is shown hereafter that the proposed approach performs much more than this simple classification by producing a rather acceptably accurate positioning in the aquarium.

Before we describe the specific actuation protocole, the classification tool that is used is first recalled in a rather general framework.

III. GENERAL FRAMEWORK

In [4], a general framework for diagnosis, classification and parameter estimation has been proposed. Validation works on some concrete engineering case studies have been reported in [5] and [6]. This section recall the underlying framework since it is in the heart of the scheme proposed in the present contribution.

A. Definitions and Notation

Let us consider a dynamic system governed by the following equations:

$$x^+ = f(x,p) \quad ; \quad y = h(x,p) \tag{3}$$

where $x \in \mathbb{R}^n$ is the state of the system, $p \in \mathbb{R}^{n_p}$ is a vector of constant parameters while y stands for the measurement vector that is assumed here to be scalar to simplify the presentation. The notation x^+ denotes the value of the state at the next sampling instant starting from the current value of the pair (x, p). The following recursive definition is used to denote the trajectory of the state for a given pair of initial state x and a parameter vector p:

$$X^{(0)}(x,p) = x \quad ; \quad X^{(i+1)}(x,p) = f\big(X^{(i)}(x,p), p\big) \tag{4}$$

Similarly, the corresponding successive measurements are denoted by $y^{(i)}(x,p) = h(X^{(i)}(x,p), p)$.

Typically, at each instant k, the estimation of the parameter vector p is based on the use of the past measurements that have been acquired during the time interval $[k-N, k]$. These measurements are gathered in a single vector $Y(k)$, namely:

$$Y(k) := \begin{pmatrix} y^{(N-1)}(x(k-N),p) \\ \vdots \\ y^{(0)}(x(k-N),p) \end{pmatrix} \in \mathbb{R}^N \tag{5}$$

B. Signature Generation

The basic intuition behind the series of works [4], [5], [6] is that since the successive measurements contained in Y uniquely determine the observable part of the state x (up to the knowledge of p), they also uniquely determine the next output y^+ (up to the knowledge of p). This intuition can be

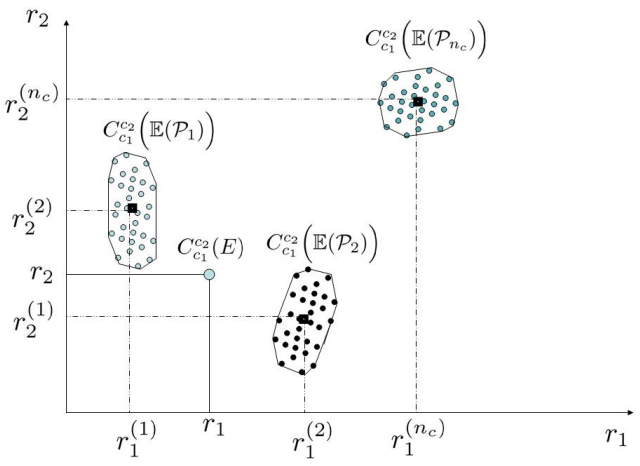

Fig. 2. Schematic view of a set of clouds representing a solved classification problem based on the subsets $\mathcal{P}_1,\dots\mathcal{P}_{n_c}$ of the parameter set values. Case where only two coordinates enable a complete solution of the classification problem. When a new experiment E is available that does not belong to the classified set, an identification is performed based on the classified classes.

summarized by the existence of some unknown function $\mathcal{F}$ satisfying:

$$y^+ = \mathcal{F}(Y, p) \tag{6}$$

Note that according to (5), Y can be viewed as a stack variable that can be updated at each sampling instant according to:

$$Y^+ = \mathcal{Q}(Y, y^+) \tag{7}$$

where $\mathcal{Q}(Y, y^+)$ is obtained from Y by removing the oldest data $y^{(0)}$ and adding the new measurement y^+ to the top of the slack.

Defining the extended state $z = (Y^T, y)^T \in \mathbb{R}^{N+1}$, one can put together equations (6) and (7) to derive the following implicit dynamical system (with completely measured state z):

$$z^+ = \mathcal{G}(z, p) \quad ; \quad z \in \mathbb{R}^{N+1} \tag{8}$$

Therefore, each measurement-based characterization (*signature*) of the unknown function $\mathcal{G}$ involved in (8) is also a characterization of the parameter vector p.

In [4], an infinite number of signatures of the unknown implicit function $\mathcal{G}$ have been proposed by defining a family of maps such that:

$$\begin{aligned} P_q : \quad \mathbb{R}^{N+1} &\to \quad \mathbb{R}^2 \\ z &\to \quad P_q(z) \end{aligned} \tag{9}$$

that associate to each measurement profile z a point in a 2D plane. The vector $q \in \mathbb{Q}$ is a vector of parameters that can be chosen to define different instantiations of the map P_q (see **Appendix A** and [4] for more details).

Now assume that an experiment is conducted with the system governed by (3) on a time interval that contains $N+M$ sampling instants. These data contains M successive values of the state z governed by (8), namely:

$$z(N+i) := \begin{pmatrix} Y(N+i) \\ y(N+i+1) \end{pmatrix} \quad i \in \{0, \dots, M-1\} \tag{10}$$

Applying successively the map P_q to the $z(N+i)$'s leads to a 2D plots (signature) defined by

$$S_q(p) := \Big\{ P_q\big(z(N+i)\big) \Big\}_{i=0}^{M-1} \subset \mathbb{R}^2 \tag{11}$$

which is clearly a graphical signature of the parameter vector p since p is involved in the definition of the system equation (8) governing the evolution of z.

C. Property of a signature

Consider a map r that associates to each graphical signature

$$S := \Big\{ (\xi_i, \eta_i) \Big\}_{i=1}^{M} \subset \mathbb{R}^2$$

a unique scalar[1]. In the sequel, such a map is called a *graphical property*. Using two pairs $c_1 := (S_{q_1}, r_1)$ and $c_2 := (S_{q_2}, r_2)$ composed each of a particular signature and an associated property, we can represent each experiments by a dot in a 2D plane $(r_1(S_{q_1}), r_2(S_{q_2}))$. That is the reason why a pair $c = (S_q, r)$ will be called a *coordinate*. Note that this 2D plane is different from the one to which belong the image of P_q. More precisely, a dot in the first 2D plane represents a point belonging to a graphical signature while a dot in the (c_1, c_2) plane represent a whole experiment through two properties of the two signatures representing this experiment.

Similarly, assuming two coordinates (c_1, c_2), a set of experiments $\mathbb{E}$ leads to a cloud $C_{c_1}^{c_2}(\mathbb{E})$ in the corresponding 2D plane $(c_1, c_2) = (r_1(S_{q_1}), r_2(S_{q_2}))$.

D. Signature Based Classification

Consider n_c subsets $\{\mathcal{P}_i\}_{i=1}^{n_c} \subset \mathbb{P}$ of the admissible set of parameters p. Assume that a set of experiments $\mathbb{E}(\mathcal{P}_i)$ is conducted for each subset $\mathcal{P}_i$ (either by changing $p \in \mathcal{P}_i$ or by changing the initial state of the system for the same p or both). These experiments form the so called *learning data* for which, the classification problem is defined as follows:

Find m coordinates $\{c_i := (S_{q_i}, r_i)\}_{i=1}^{m}$ such that the following property is satisfied: For all subset index $\imath \in \{1, \dots, n_c\}$, there exists a pair of coordinates (c_1, c_2) such that the two clouds:

$$C_{c_1}^{c_2}\big(\mathbb{E}(\mathcal{P}_i)\big) \quad \text{and} \quad C_{c_1}^{c_2}\big(\mathbb{E}(\mathcal{P}_j)\big)$$

are separated for all $j \neq \imath$. The set of all such pairs (c_1, c_2) will be denoted hereafter by $Dis(\imath)$

---

[1]This may be $\max_i(\xi_i)$, $\max_i(\eta_i) - \min_i(\eta_i)$, $mean(\{\xi_i\}_{i=1}^N)$, $std(\{\eta_i\}_{i=1}^N)$, $\max_i(\{\frac{\xi_i}{(\varepsilon+|\eta_i|)}\})$, …, etc.

E. Solving the classification problem

Based on the above separation condition, an optimization software has been recently developed[2] to solve the classification problem. This is done by a stochastic search (over the set of signature parameters (q, N) and a pre-defined set of graphical properties) that aims at achieving a pre-specified separation level $d_{min} > 0$. As soon as a pair (c_1, c_2) is found that *isolates* a subset of the configurations $\{\mathcal{P}_i\}_{i=1}^{n_c}$ to be classified, these configurations are removed from the list and the search continues while focusing on the remaining ones until the list is empty (the classification problem is solved).

F. Estimation of p

The parameter estimation is made easier when there is a solution to the classification problem that meets the following requirements:

There are two coordinates c_1 and c_2 that completely solve the classification problem. Namely, the classification problem admits at least one solution with $m = 2$.

Under this assumption, one obtains the situation depicted on Figure 2. Namely, the clouds $C_{c_1}^{c_2}(\mathbb{E}(\mathcal{P}_i))$ representing the $2D$ representation of the set of experiments $\mathbb{E}(\mathcal{P}_i)$ for $i = 1, \ldots, n_c$ form n_c separated sets. When the measurements of a new experiment E are acquired, the corresponding dot $r := (r_1, r_2) = C_{c_1}^{c_2}(E)$ is computed and the estimation of the corresponding parameter value $\hat{p}$ is obtained according to:

$$\hat{p} = \sum_{i=1}^{n_c} \phi_i(r) \cdot p^{(i)} \tag{12}$$

where $p^{(i)}$ is a representative value of the parameter values that have been used in the generation of the experiments contained in $\mathbb{E}(\mathcal{P}_i)$ while the $\phi_i(\cdot)$'s are appropriate weighting functions such that $\sum_{i=1}^{n_c} \phi_i(r) = 1$.

IV. Application to Electrolocation

In this section, the application of the proposed methodology to the electrolocation problem described in section II is shown. Note that because of symmetry, we consider only the triangular domain ABC depicted on Figure 3.(a) since otherwise, ambiguity is unavoidable.

A. Available Measurements

Figure 3.(b) shows a set of positions $\{(x_i, y_i)\}_{i=1}^{21}$ where measurements are acquired for design and/or validation purposes according to the following protocole: For each $i \in \{1, \ldots, 21\}$, the sensor is positioned at (x_i, y_i) and a $360\,\mathrm{deg}$ rotation at constant angular velocity is performed starting form some initial value θ_j and the corresponding measurements are acquired forming the experiment that will denoted hereafter by E_i^j. Moreover, in order to be insensitive to the value of the initial angular position,

[2]See http://www.mazenalamir.fr/DiagSign/ for the description of the software. See also http://www.mazenalamir.fr/files/APP_diagsign.jpg for the software protection licence.

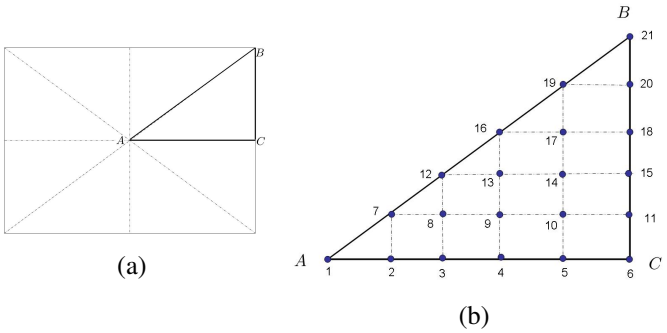

Fig. 3. (a) Because of symmetry, only the triangle ABC is considered. (b) The set of different positions where measurement are acquired for design and/or validation

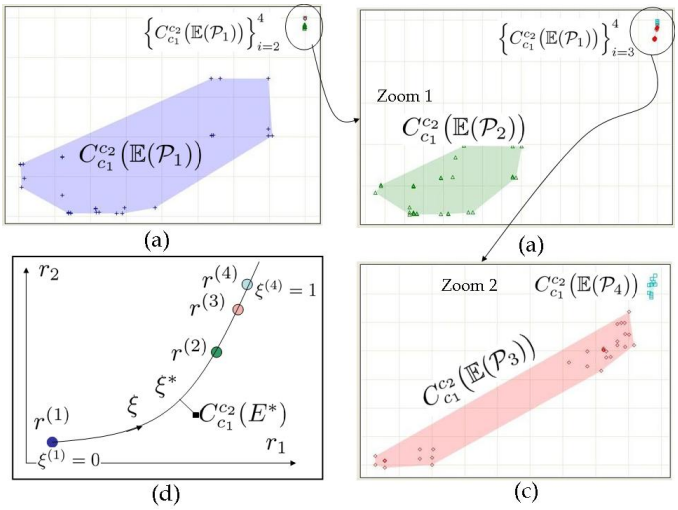

Fig. 4. Signature based solution of the x-classification problem. The clouds $C_{c_1}^{c_2}(\mathbb{E}(\mathcal{P}_i))$ are clearly separated for $i \in \{1, \ldots, 4\}$: (a) overall view of the clouds position. (b) zoom excluding the first cloud. (c) zoom excluding the first two clouds. (d) Principle of the estimation $\hat{x}(E^*)$ corresponding to a new experiment E^* according to equation (17)

$n_{exp} = 10$ different values of the initial angular positions θ_j uniformly distributed on $[0, 360]$ are used leading to 10 different experiments $\{E_i^j\}_{j=1}^{n_{exp}=10}$ for each position (x_i, y_i).

In what follows, it is shown how the general framework of section III can be used to compute an estimation of the position (x, y) by performing a simple $360\,\mathrm{deg}$ rotation experiment on line. It is in particular shown that this can be done in two successive steps, the first leading to an estimate $\hat{x}$ of x and the second to an estimate $\hat{y}$ of y given $\hat{x}$.

B. Estimating the x coordinate

In order to estimate the coordinate x, the framework proposed in the preceding sections is used with the following instantiations:

- $n_c = 4$ learning subsets are used such that
- $\mathcal{P}_1 = \{x_6\}$, $\mathcal{P}_2 = \{x_5\}$, $\mathcal{P}_3 = \{x_3\}$ and $\mathcal{P}_4 = \{x_1\}$

- The experiments $\mathbb{E}(\mathcal{P}_i)$ are defined as follows:

$$\mathbb{E}(\mathcal{P}_1) = \left\{\{E_i^j\}_{j=1}^{10}\right\}_{i\in\{6,15,20,21\}} \quad (13)$$

$$\mathbb{E}(\mathcal{P}_2) = \left\{\{E_i^j\}_{j=1}^{10}\right\}_{i\in\{5,14,19\}} \quad (14)$$

$$\mathbb{E}(\mathcal{P}_3) = \left\{\{E_i^j\}_{j=1}^{10}\right\}_{i\in\{3,8,12\}} \quad (15)$$

$$\mathbb{E}(\mathcal{P}_4) = \left\{\{E_i^j\}_{j=1}^{10}\right\}_{i\in\{1\}} \quad (16)$$

  which clearly shows that only 11 of the 21 positions are used in the learning phase (50% of the available data). The remaining points are used for the validation of the extrapolation capacity of the resulting algorithm.

Using the above choices, the resulting classification problem has been submitted to DIAGSIGN and the classification problem has been solved as shown on Figure 4. Indeed, the results coincides with the general scheme depicted in Figure 2 since the clouds representing the different subsets of values of x are clearly separated.

Denoting by $r^{(i)} = (r_1^{(i)}, r_2^{(i)})$ the coordinates of the centers of the convex hulls of the clouds $C_{c_1}^{c_2}(\mathbb{E}(\mathcal{P}_i))$, one can define a smooth spline $r(\xi)$ in the curvilinear abscissa ξ linking the centers $\{r^{(i)}\}_{i=1}^{n_c=4}$. When data from a new experiment E^* is available (see Figure 4.d), the corresponding dot is computed, its projection on the median line is obtained that determines the corresponding curvilinear abscissa ξ^*. The spline is then used to compute the estimation of x according to:

$$\hat{x}(E^*) = \left[\frac{\xi^{(i+1)} - \xi^*}{\xi^{(i+1)} - \xi^{(i)}}\right] \cdot x_i + \left[\frac{\xi^* - \xi^{(i)}}{\xi^{(i+1)} - \xi^{(i)}}\right] \cdot x_{i+1} \quad (17)$$

where (i) and $(i+1)$ are the indices of the clouds that surround the new experiment dot $C_{c_1}^{c_2}(E^*)$ along the curvilinear mean line.

C. Estimating the y coordinate

The estimation of y is done using the following steps:

- First, three classification subproblems are solved using the same methodology explained above for the x-coordinates case. These three problems correspond each to a given x and for which different $p = y$ level are used to define the subsets to be discriminated. The definition of n_c and the subsets $\mathcal{P}_i$ for each of these subproblems are depicted on Figure 5. It is worth underlying that only the experiment used in the x-classification are used here so that only 50% of the available data are used in the learning process.

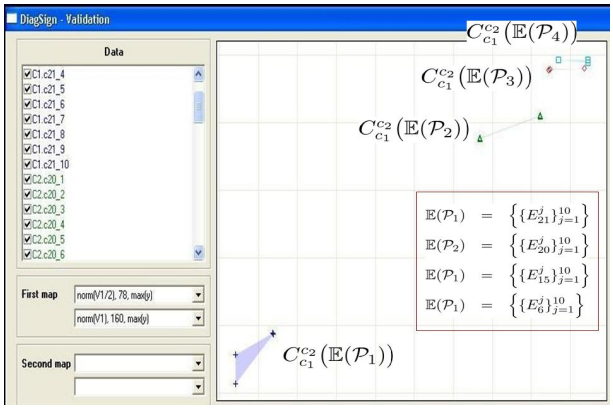

(a)

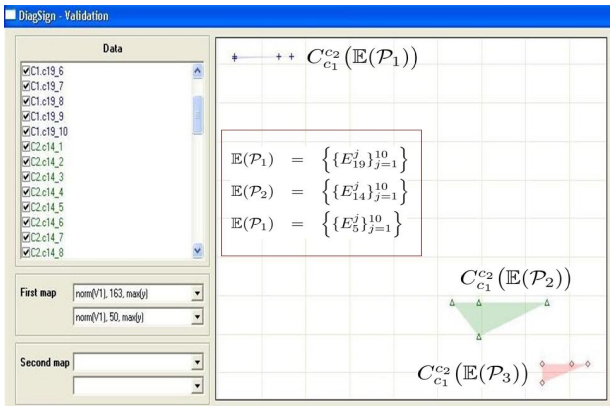

(b)

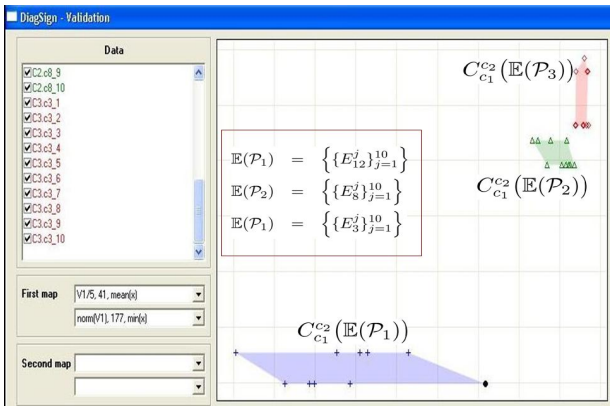

(c)

Fig. 5. The three y-classification subproblems used to perform the conditional estimation of y when (a) $x = x_6$, (b) $x = x_5$ or (c) $x = x_3$. The definition of the subset of $p = y$ used for each subproblem definition is given on each corresponding sub-figure.

Note that the y-classification subproblems are defined for $x = x_6$, $x = x_5$ and $x = x_3$. Therefore, once these subproblems are solved and using the same interpolation formulae (17), one disposes of the following conditional estimators:

$$\hat{y}(E^*|x = x_6) \quad ; \quad \hat{y}(E^*|x = x_5) \quad ; \quad \hat{y}(E^*|x = x_3)$$

which produce the estimation of y provided that x belongs to the set $\{x_6, x_5, x_3\}$. Note also that one disposes of the trivial estimator $\hat{y}(E^*|x = x_1) = 0$.

- When data corresponding to a new experiment E^* is available, the estimation $\hat{x}(E^*)$ is first computed, then the bounds

$$(x_{min}(E^*), x_{max}(E^*)) \in \{x_1, x_3, x_5, x_6\}^2$$

are computed such that:

$$x_{min}(E^*) \leq \hat{x}(E^*) \leq x_{max}(E^*) \tag{18}$$

- Finally, the estimated value $\hat{y}(E^*)$ is given by:

$$\hat{y}(E^*) := \left[\frac{x_{max}(E^*) - \hat{x}(E^*)}{x_{max}(E^*) - x_{min}(E^*)}\right] \cdot \hat{y}(E^* | x_{min}(E^*)) + \left[\frac{\hat{x}(E^*) - x_{min}(E^*)}{x_{max}(E^*) - x_{min}(E^*)}\right] \cdot \hat{y}(E^* | x_{max}(E^*)) \tag{19}$$

D. Validation results

The estimation laws (17) and (19) are used here on the entire set of experimental points to validate their extrapolation power on those experiments that have not been included in the learning phase. The results are shown on Figure 6 where the estimation error for each (x, y) position are graphically represented by ellipses.

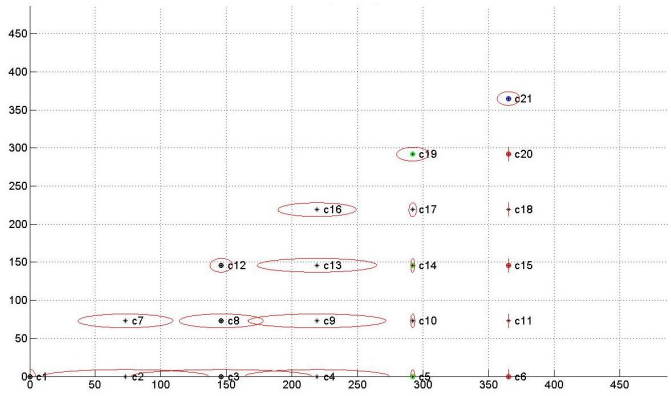

Fig. 6. View of the estimation error when the estimation laws (17) and (19) are applied to the whole experimental set of data. Recall that the learning phase uses only 11 of the 21 where the probe has been position and measurement data are acquired. Note in particular that the points $\{2, 7, 4, 9, 13, 16, 10, 17, 11, 18\}$ are not used in the learning phase.

Note that the points belonging to the set:

$$\{2, 7, 4, 9, 13, 16, 10, 17, 11, 18\}$$

have not been used in the learning phase. This shows a remarkably nice extrapolation power of the proposed strategy. Note also that the precision increases when the probe approaches the wall in accordance with the observations already invoked by [7].

V. Conclusion

In this paper, a preliminary validation of a model-free electrolocation methodology has been proposed and experimentally validated. Future investigation will address the navigation in the presence of arbitrary obstacles where the classification problem would be defined by the presence or not of obstacles in such or such direction. These directions are defined in the robot reference frame. In that sense, the ambition of absolute positioning will be dropped towards a more realistic eletrolocation context. Moreover, the use of multiple electrodes probes (up to 16 already available on a single probe) would avoid the need for a rather involved rotating protocole.

Appendix

A. Expression of the map $P_q(z)$

Given $z \in \mathbb{R}^{N+1}$, the following map has been suggested in [4]:

$$P_q(z) = \Phi_0(z) + \lambda(z) \cdot \Big[\Phi_1(z) - \Phi_0(z)\Big] \tag{20}$$

$$\Phi_0(z) = \frac{1}{2N} \sum_{j=1}^{N} \Psi_j(z) \tag{21}$$

$$\Phi_1(z) = \frac{1}{2N} \sum_{j=1}^{N} \bar{Z}_j \Psi_j(z) \tag{22}$$

where

$$\Psi_j(z) := \Big[(1 + \bar{Z}_i)Q_{i+1} - (\bar{Z}_i - 1)Q_i\Big]$$

$$\bar{Z}_i := \frac{z_i}{\eta_n \cdot \max_{j=1}^{N} |z_i| + 1}$$

$$Q_i := \Big(\cos(\tfrac{2\pi(i-1)}{N}), \sin(\tfrac{2\pi(i-1)}{N})\Big)^T$$

$$\lambda(z) := \frac{z_{N+1}}{\eta_n \cdot \max_{j=1}^{N} |z_i| + 1} - \frac{1}{N} \sum_{i=1}^{N} \bar{Z}_i$$

The vector of signature parameter q include the integer N, the normalization coefficient $\eta_n \in \{0, 1\}$ and the under-sampling integer that is not mentioned in the equation for simplicity.

References

[1] W. Heiligenberg "Electrolocation of Objects in the Electric Fish *Eigenmannia* (Rhamphichthiade Gymnotoidei) ", *J. Comp. Physiol.*, Vol. 87, pp. 137-164, 1973.

[2] G. Von der Emde, S. Schwarz, L. Gomez, R. Budelli and K. Grant "Electric Fish Measure Distabce in The Dark", *Letters to Nature*, Vol. 395, pp. 890-894, 1998.

[3] M. Maciver and M. E. Nelson "Towards Biorobotic Electrosensory System", *Autonomous Robots*, Vol. 11, pp.263-266, 2001.

[4] B. Youssef and M. Alamir "Generic signature based tool for diagnosis and parametric estimation for multi-variable dynamical nonlinear systems", *Proceedings of the 42th Conference on Decision and Control*, Hawaï, USA. 2003.

[5] B. Youssef and M. Alamir "Diagnosis and On-line parametric estimation of automotive electronic throttle control system", *Proceedings of the IFAC World Congress*, Praha, Czech Republic, July 2005.

[6] B. Youssef, M. Alamir and F. Ibrahim "Diagnosis and on-line parametric estimation of simulated moving bed", *Proceedings of the 44th Conference on Decision and Control (CDC-ECC'05)*, Seville, Spain, 2005.

[7] G. Baffet, F. Boyer and P. B. Gossiaux "Biomimetic localization using the electrolocation sens of the electric fish", *Proceedings of the 2008 IEEE International Conference on Robotics and Biomimetics*, Bangkok, Thailand, February 21-26, 2009.

[8] R. Williams, B. Rasnow and Ch. Assad "Hypercube Simulations of Electric Fish Potentials", *In Wakler, D. (Ed.), Proc. Fifth Distributed Memory Computing Conference, Charleston, SC.* 1990.